



NONLINEAR BEHAVIOR OF REINFORCED CONCRETE STRUCTURES CONSIDERING BOND-SLIP UNDER CORROSION

S. Abtahi⁽¹⁾, Y. Li⁽²⁾

⁽¹⁾ Ph.D. Student, Dept. of Civil and Environmental Eng., University of Alberta, abtahi1@ualberta.ca

⁽²⁾ Assistant Professor, Dept. of Civil and Environmental Eng., University of Alberta, yong9@ualberta.ca

Abstract

This paper studies the nonlinear behavior of reinforced concrete (RC) structures with corrosion-affected deterioration. In order to consider the imperfect bonding between concrete and steel in RC structures, an efficient finite element model, which is capable of capturing bond-slip, needs to be employed. To this end, a new fiber beam-column element with nonlinear bond-slip is implemented in OpenSees. In this element, geometrical nonlinearity is considered for both the steel rebars and concrete beam components using the corotational formulation for rebars and concrete beam components simultaneously. This finite element formulation is employed to study the effect of deteriorated bonding due to corrosion on the strength/deformation capacity and energy dissipation of the monotonic and cyclic behavior of RC columns. The simulation results indicate when the bonding is degraded, the strength capacity, deformation capacity, and energy dissipation of RC structures would decrease compared to the as-built condition. All of the results reaffirm that the performance of RC structures can be significantly altered by corrosion-induced deterioration due to aging.

Keywords: Nonlinear behavior; Reinforced concrete structures; Steel corrosion; Fiber beam-column element with bond-slip.

1. Introduction

The seismic performance of reinforced concrete (RC) structures has been a research focus in the field of structural and earthquake engineering. However, the majority of the efforts is dedicated to the RC structures without considering the deterioration due to aging in aggressive environmental conditions. For example, chloride contamination in RC structures, due to using de-icing salts and environmental conditions (e.g., in the coastal areas), can lead to various deteriorations, including concrete cover cracking or spalling, reduction of the cross-sectional area, loss of confinement, loss of bonding strength, etc. Such deteriorations will in turn affect the seismic performance of RC structures.

Several past studies (e.g., [1, 2]) focused on time-dependent corrosion models to quantify the steel mass loss as a measure of corrosion level. Recognizing this, several researchers started to look into the effect of corrosion-induced deteriorations at the structural component or system level (e.g., [2, 3]). In most of those studies, a common assumption is perfect bonding (i.e., strain compatibility) between the corroded reinforcing steel and the surrounding concrete. To reveal the true performance of corroded structures, it is important to model corroded bond-slip in structural analysis as implied in some studies (e.g., [4, 5]). However, in the aforementioned studies, over-simplified modeling approaches were used to consider imperfect bonding, which are inappropriate to investigate the effect of corroded bond-slip in detail. This is because the corrosion-affected bonding needs to be modeled explicitly and efficiently in order to study the effect of corrosion on structural performance degradation, particularly when uncertainty is considered.

As such, an enhanced fiber beam-column element considering bond-slip and corroded bond-slip material models are implemented in the open-source finite element software framework, OpenSees [6]. The importance of bond-slip has been evidenced in experimental tests of uncorroded structural components with normal bonding, showing that the force-deformation behavior is characterized by pinched hysteresis with



less energy dissipation capabilities compared to the perfect bonding case [7]. To consider imperfect bonding, which is to capture the relative slip between the steel and concrete, different modeling strategies have been proposed in the literature. Several approaches aim to take into account the rebar slippage in the anchored region by either using a zero-length element [8], modifying the stress-strain behavior of steel [9], or altering the composite behavior of steel and concrete at the section level [10]. The first two methods did not explicitly consider the bonding behavior (i.e., stress-slip), and thus cannot be appropriately approached by incorporating the corroded bonding into structural models. In contrast, the third approach allows explicit bond-slip behaviors but is limited to considering the anchorage slippage only (e.g., in the column footing). Namely, this approach cannot be applied to corroded structures since corroded bonding needs to be modeled for the unanchored region (e.g., column above the footing), where corrosion is relatively more common and severe than the anchored region. As such, the displacement-based fiber beam-column element with bond-slip proposed by [11] is adopted in this study with further improvement. In this element, the explicit bond-slip relationship can be considered for the entire structural member because the relative slip is introduced by using additional degrees of freedom (DOFs) for rebar movements. Note that the original formulation of the element is based on linear geometry transformation, while it is enhanced in this study to take into account geometrical nonlinearity through corotational formulation. As required in the newly implemented fiber beam-column element, various bond-slip models are available in the literature for normal bonding (e.g., [12, 13]) and for corroded bonding (e.g., [4, 14]). In this study, the well-received bond-slip models, proposed in [12] and [4], are used for the uncorroded and corroded cases, respectively.

The remainder of this paper is organized as follows. The enhanced displacement-based fiber beam-column element and bond-slip material models are firstly described. Using the newly implemented element and bond-slip material models, one uncorroded and one corroded columns are modeled and the simulation results are compared with experimental data for the purpose of validation. Based on the model developed, a parametric study on the structural performance of an RC column under monotonic and cyclic loads is conducted by varying the corrosion levels (i.e., age-related). The degraded performance of the RC columns due to corroded bonding is investigated with comparison to the effect of corrosion-induced steel section loss, which is commonly considered in other studies. Note that the other possible effects of corrosion on concrete cracking and spalling are not considered in the parametric study here.

2. Displacement-Based RC Frame Element with Bond-Slip

This section revisits the displacement-based fiber beam-column (i.e., frame) element formulation considering the imperfect bonding between concrete and rebars. This element initially presented in [11] considers rebars as truss-like members with individual DOFs to permit the slip in the context of linear geometry (i.e., no geometric nonlinearity). In the following, the element formulation is briefly reviewed and then, the newly developed coordinate transformation to consider the effect of nonlinear geometry is introduced.

2.1 Element formulation

The two-dimensional (2D) RC frame element with n rebars consists of a two-node beam with six conventional DOFs (i.e., axial, transversal, and rotational) representing the concrete beam and another $2n$ DOFs to consider the movement of steel rebars with slippage. Fig. 1 shows the two-node beam with the concrete part indicated by the solid gray area and for the steel reinforcement part indicated by the hatched area. The element nodal displacement vector \mathbf{U} is $\{u_1 \ u_2 \ u_3 \ \bar{u}_1^1 \ \dots \ \bar{u}_1^n \ u_4 \ u_5 \ u_6 \ \bar{u}_2^1 \ \dots \ \bar{u}_2^n\}$, and the augmented section displacement vector $\mathbf{u}(x) = \{u_B(x) \ v_B(x) \ \bar{u}_1 \ \dots \ \bar{u}_1 \ \dots \ \bar{u}_n \ \dots \ \bar{u}_n\}$. Accordingly, the augmented section deformation vector $\mathbf{d}(x) = \{\varepsilon_B(x) \ \kappa_B(x) \ \varepsilon_1(x) \ \dots \ \varepsilon_i(x) \ \dots \ \varepsilon_n(x)\}$ is related to the augmented section displacement vector through compatibility equations, in which the section axial strain $\varepsilon_B(x) = du_B(x)/dx$, the section curvature $\kappa_B(x) = d^2v_B(x)/dx^2$, and the axial strain of the i^{th} rebar $\varepsilon_i = d\bar{u}_i(x)/dx$. Accordingly, the slip field of the i^{th} rebar, $u_b^i(x)$, is described as:

$$u_b^i(x) = \bar{u}_i(x) - (u_B(x) - \frac{dv_B(x)}{dx} \bar{y}_i) \quad (1)$$



where \bar{y}_i is the distance of the i^{th} rebar from the reference axis.

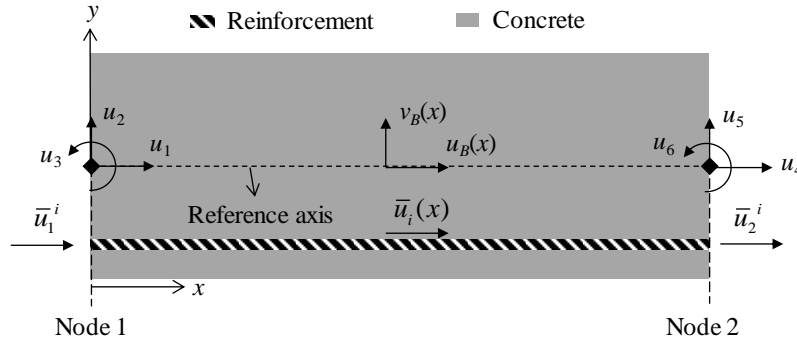


Fig. 1 – Schematic view of the RC frame element considering bond-slip

The nodal displacements are used to characterize the element displacement fields through shape functions $\mathbf{N}(x)_{(2+n) \times (6+2n)} = \{\mathbf{N}_{B1}(x)_{2 \times 3} \mathbf{0}_{2 \times n} \mathbf{N}_{B2}(x)_{2 \times 3} \mathbf{0}_{2 \times n}; \mathbf{0}_{n \times 3} \mathbf{N}_{b1}(x)_{n \times n} \mathbf{0}_{n \times 3} \mathbf{N}_{b2}(x)_{n \times n}\}$, in which $\mathbf{N}_B(x) = \{\mathbf{N}_{B1}(x) \mathbf{N}_{B2}(x)\}$ is formed based on the conventional linear shape functions for the axial displacement field and Hermite shape functions for the transverse displacement field for concrete, and $\mathbf{N}_{b1}(x)$ as well as $\mathbf{N}_{b2}(x)$ is formed based on linear shape functions for the axial displacement fields of rebars with bond-slip. As a result, the augmented section deformation vector $\mathbf{d}(x)$ and slip vector $\mathbf{d}_b(x)$ for an RC frame element with n rebars can be written as:

$$\mathbf{d}(x) = \begin{bmatrix} \varepsilon_B(x) \\ \kappa_B(x) \\ \bar{\varepsilon}_1(x) \\ M \\ \bar{\varepsilon}_i(x) \\ M \\ \bar{\varepsilon}_n(x) \end{bmatrix} = \begin{bmatrix} d/dx & 0 & 0 & L & 0 \\ 0 & d^2/dx^2 & 0 & L & 0 \\ \hline 0 & 0 & d/dx & L & 0 \\ M & M & M & O & M \\ 0 & 0 & 0 & L & d/dx \end{bmatrix} \mathbf{N}(x)\mathbf{U} = \mathbf{B}(x)\mathbf{U} \quad (2)$$

and

$$\mathbf{d}_b(x) = \begin{bmatrix} u_b^1(x) \\ M \\ u_b^n(x) \end{bmatrix} = \begin{bmatrix} -1 & \bar{y}_1 \frac{d}{dx} & 1 & L & 0 \\ M & M & M & O & M \\ -1 & \bar{y}_n \frac{d}{dx} & 0 & L & 1 \end{bmatrix} \mathbf{N}(x)\mathbf{U} = \mathbf{B}_b(x)\mathbf{U} \quad (3)$$

Corresponding to the augmented section deformation vector $\mathbf{d}(x)$, the augmented section force vector $\mathbf{D}(x)$ is defined as $\{N_B(x) M_B(x) \bar{N}_1(x) \dots \bar{N}_i(x) \dots \bar{N}_n(x)\}$, in which $N_B(x)$ is the axial force and $M_B(x)$ is the bending moment contributed from the concrete part, and $\bar{N}_i(x)$ is the axial force in the i^{th} rebar. To describe the bonding stresses $t_i(x)$ between the i^{th} rebar and the surrounding concrete, $\mathbf{D}_b(x) = \{p_1 t_1(x) \dots p_i t_i(x) \dots p_n t_n(x)\}$ is used, where p_i is the perimeter of the i^{th} rebar. With the displacement fields defined, the principle of virtual work is used to derive the element stiffness matrix and the resisting force for displacement-based element. The element stiffness matrix $\mathbf{K}_{(6+2n) \times (6+2n)}$ is assembled by considering the contributions from both the concrete and steel rebars with bond-slip. The element forces $\mathbf{P}_{(6+2n) \times 1}$ can also be determined similarly (see [11]).

Following the formulation briefly described, a displacement-based fiber beam-column element with bond-slip (i.e., *dispBeamColumnBS*) is implemented in OpenSees, in conjunction with the newly implemented fiber section model for the section state determination (i.e., *FiberBSele*), and bond-slip model



for material state determination. Note that the material nonlinearities are considered in the formulation of the \mathbf{K} , and the geometrical nonlinearity will be addressed in the next section.

2.2 Nonlinear geometry

To capture the effect of geometrical nonlinearity, the hybrid corotational transformation is employed for the frame element described earlier. In this regard, different corotational transformations are incorporated for the concrete part and the steel rebars. To be specific, for representing concrete deformations, the conventional corotational transformation for beam elements without bond-slip [15] is used. As shown in Eq. (4), the DOFs in the local coordinate system for concrete deformations are related to the DOFs in the basic system (see Fig. 2).

$$\begin{aligned}\Delta_1 &= \sqrt{(L_0 + u_4 - u_1)^2 + (u_5 - u_2)^2} - L_0 \\ \Delta_2 &= u_3 - \arctan\left(\frac{u_5 - u_2}{L_0 + u_4 - u_1}\right) \\ \Delta_3 &= u_6 - \arctan\left(\frac{u_5 - u_2}{L_0 + u_4 - u_1}\right)\end{aligned}\quad (4)$$

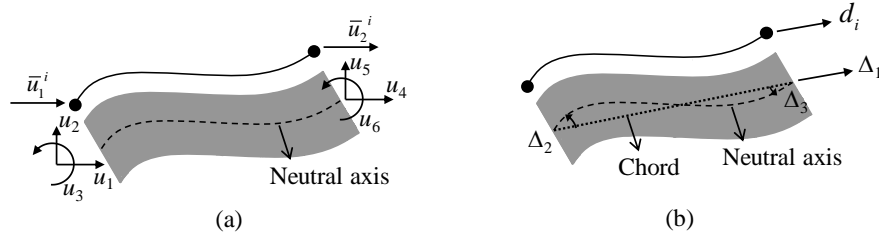


Fig. 2 – Coordinate transformation: (a) local system and (b) basic system

For the DOFs representing steel rebar deformations, the conventional corotational transformation for truss elements [16] is employed by relating the one axial DOF d_i for the i^{th} rebar in the basic system to the corresponding DOFs in the local system according to Eq. (5):

$$d_i = \sqrt{(L_0 + \bar{u}_2^i - \bar{u}_1^i)^2 + (u_5 - u_2)^2} - L_0 \quad (5)$$

By defining the nonlinear relationships, see Eqs. (4) and (5), between the DOFs in the basic system and the DOFs in the local system, the corotational transformation matrix can thus be derived. As such, a new geometrical transformation (i.e., *corotationalBS*) to consider the effect of nonlinear geometry is implemented in OpenSees for the newly implemented fiber beam-column element with bond-slip.

3. Bond-Slip Models

3.1 Normal bond-slip

The slippage between steel rebars and the surrounding concrete can severely affect the behavior of uncorroded RC structures. In order to consider the normal bond-slip (i.e., no corrosion effect), many studies have proposed different bond-slip models, defined as the relationship between the bonding stress and the slippage displacement, based on experimental data. Among them, a commonly used bond-slip model proposed by [12] is employed in this study to validate the finite element model developed for the uncorroded RC column using the newly implemented fiber beam-column elements with bond-slip and geometric transformation. In this bond-slip model, the backbone curve of the bonding stress-slip relationship starts with a nonlinear (or linear as a special case) curve, characterized by a power-law relationship with a nonlinearity parameter α , until it reaches the maximum bond stress, t_1 , at the slip u_1 . After this point, as the slip increases, the bond stress remains constant. When the slip continues increasing and gets greater than u_2 , the bonding



starts softening (e.g., due to the crushing of the concrete between lugs), in which the bond stress would decrease linearly until reaching the critical point (u_3, t_3). After this point, the bond stress stays equal to t_3 as commonly referred as the residual friction branch. This model is demonstrated in Fig. 3(a), where a linear ascending branch is considered with the value of $\alpha = 1$. Note that the model parameters u_1, u_2, u_3, t_1, t_3 , and α depend on the properties of the steel reinforcement, concrete, etc. [12, 13].

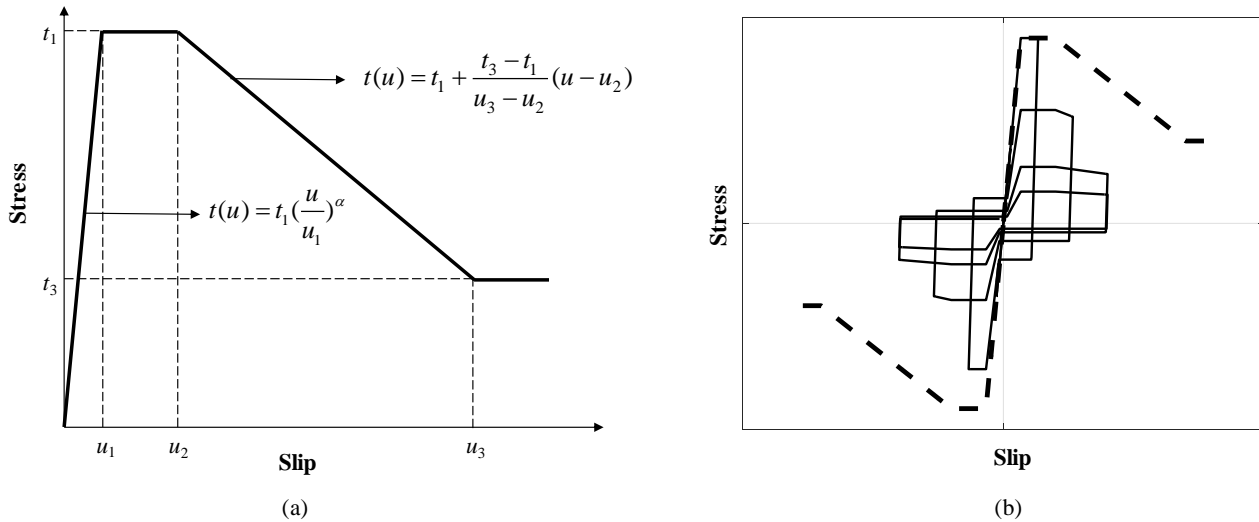


Fig. 3 – Schematic bond-slip material behavior: (a) monotonic and (b) cyclic behavior

Fig. 3(b) shows the general cyclic behavior of the bond-slip model adopted in this study. It is mainly characterized by the initial envelope, unloading/reloading with a relatively high stiffness equal to multiples of the secant stiffness corresponding to the point (u_1, t_1) such as $4t_1/u_1$ [13], the friction branch, and reduced envelope due to accumulative damage during cycling. To account for such envelope reduction, two damage factors are used in the model: one based on the total dissipated energy to reduce the envelope and the other one based on the energy dissipated by the friction branch only to update friction stress level [12]. To show the effect of the accumulative damage caused by cycling in the friction branch and reduced monotonic envelope, several hysteresis loops are plotted in Fig. 3(b) with comparison to the initial envelope indicated as the dashed line.

3.2 Corroded bond-slip

For corroded RC structures, the bond-slip behavior affected by the rebar corrosion will further modify the structural behavior. Few models exist for the cyclic bond-slip behavior of corroded rebars, and this study integrates the existing normal bond-slip model with corrosion-induced damage factors proposed by [4] for the corroded bond-slip. The first corrosion-induced damage factor shown in Eq. (6) is to quantify the effect of corrosion on t_1 as the ratio between the corroded t_1 , denoted as t_1^c , and the initial uncorroded t_1 , denoted as t_1^0 . Here, the corrosion level, K , is measured as the percentage of mass loss ratio. Note that for corrosion level under 3%, the effect of corrosion on t_1 is neglected.

$$\frac{t_1^c}{t_1^0} = \begin{cases} 1.2e^{-0.076K} \leq 1.0 & K > 3\% \\ 1.0 & K \leq 3\% \end{cases} \quad (6)$$

The other corrosion-induced damage factor is to consider the effect on the residual friction branch. It is defined as the ratio between the corroded t_3 , denoted as t_3^c , and t_1^c , shown in Eq. (7).



$$\frac{t_3^c}{t_1^c} = \begin{cases} 0.26 + 0.13K & 0 \leq K < 3\% \\ 0.65 & 3\% \leq K < 13\% \\ 0.65 - 0.06(K - 13) & 13\% \leq K < 20\% \\ 0.23 & K \geq 20\% \end{cases} \quad (7)$$

Note that experimental studies indicated that the influence of corrosion on the slip values of u_1 , u_2 , and u_3 is negligible [4] and thus not considered here.

Concerning the corrosion effect on the cyclic bond-slip behavior, the two cumulative damage factors, which are dependent on the total energy dissipation and the energy dissipated by the friction branch, are thus affected by the corrosion level. Hence, two new cumulative damage factors are used to consider the effect of corrosion on the cyclic behavior of bond-slip. Readers of interest can refer to [4] for further details.

The normal and corroded bond-slip material models presented above are implemented in OpenSees as *BondSlip03* and *BondSlipCorU*, respectively. Together with the newly implemented element with bond-slip (i.e., *dispBeamColumnBS*), fiber section (i.e., *FiberBSele*), and geometrical transformation (i.e., *corotationalBS*), this equips OpenSees with a versatile and efficient FE modeling module, which is missing in the current literature for efficient modeling of corroded RC frame structures.

4. FE Model Development and Validation

The newly developed and implemented FE modeling capabilities in OpenSees are used to develop numerical models for existing RC columns tested in the literature. One uncorroded and one corroded RC columns identified with the observable effect of bond-slip are used for the validation purpose.

4.1 Uncorroded RC column

The uncorroded RC column considered here is a column with square cross-section [17], denoted as Bousias column, as shown in Fig. 4(a) with geometrical and section properties. Note that the bond-slip properties provided by [18] are used for the Bousias column. For this uncorroded RC column, the static cyclic pushover analysis has been conducted with both perfect and normal bonding and then the results are compared to the experimental data.

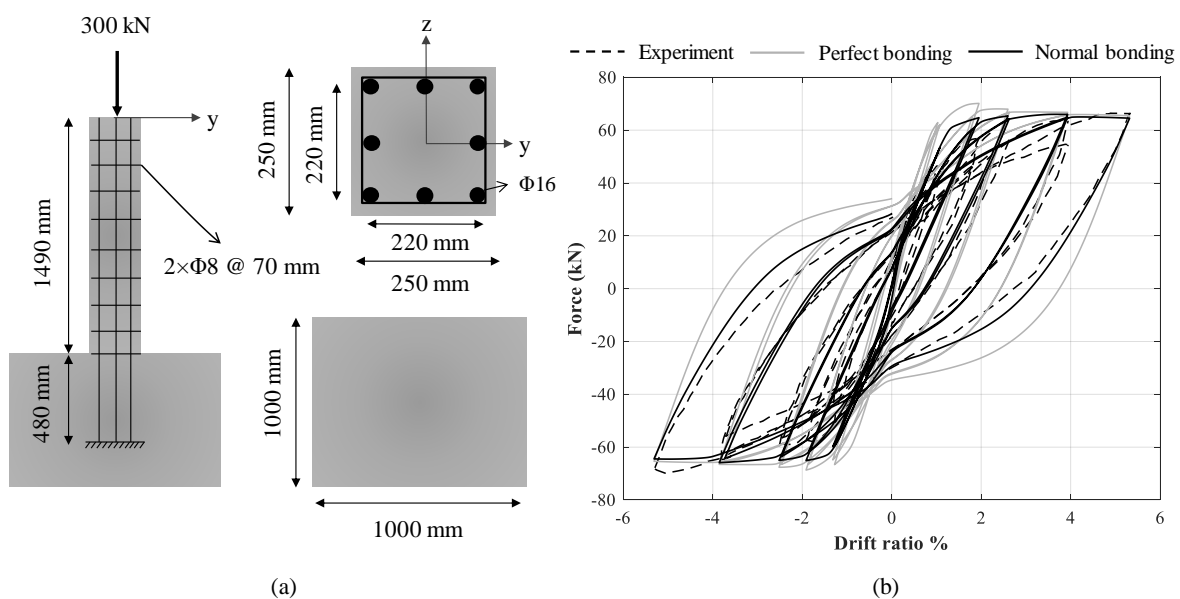


Fig. 4 – (a) Geometry, sections, and axial load, and (b) force-drift ratio hysteresis comparison between FE prediction and experiment for the uncorroded RC column: Bousias column



Fig. 4(b) shows the lateral force-drift ratio hysteresis for the Bousias column simulated with perfect (i.e., indicated by gray solid) and normal bonding (i.e., indicated by black dashed), compared to the experimental results (i.e., indicated by black solid). A reasonably better agreement with the experiments can be achieved for the column modeled using fiber beam-column elements with normal bonding when compared with the case of perfect bonding. In particular, normal bonding allows capturing the pinching behavior in the hysteretic loops well.

4.2 Corroded RC column

The corroded RC column considered for validation is a column under artificial corrosion in the laboratory, denoted as Meda column [19]. The geometry and section properties of this column are shown in Fig. 5(a). This column was artificially corroded with a mass loss ratio (i.e., corrosion level) equal to 20% and then, the static cyclic pushover test was conducted. In this study, a finite element model is developed for this column using the newly implemented fiber beam-column element as well as the corroded bond-slip model presented earlier. Note that in order to model this corroded column, several relevant aspects related to the effect of corrosion are considered. First of all, because of the volumetric expansion coming from the corroded steel, the concrete cover would be cracked and spalled. As a result, the strength of concrete is reduced [20] accordingly. Secondly, the rebar area is decreased based on the mass loss ratio and also, due to pitting corrosion, the steel strength is degraded [21]. Thirdly, the confined concrete properties are updated through Mander's equations [22] to consider the corrosion effect on the confinement. Finally, the corroded bond-slip is represented based on the described model in the previous section. With the developed finite element model, a cyclic pushover analysis is performed following the loading protocol in the test. The resulted force-drift ratio hysteresis is presented in Fig. 5(b) with the gray solid and the black solid curves predicted from the finite element model with perfect bonding and normal bonding, respectively, in comparison with the experimental result indicated by the black dashed curve. Before reaching the deformation level with a drift ratio of 2.0%, the model predictions correlated well with the experimental results when corroded bond-slip is considered. In terms of the pinching behavior (or less energy dissipation) characterized for the effect of the bond-slip, it can be concluded that the model successfully captures the effect of corroded bond-slip. Note that the strength degradation at large deformation levels is not captured, and this stems from the fact that the reinforcement is buckled in this test [19] while the effect of buckling is not considered in the current steel model used, i.e., steel02 in OpenSees. Further inclusion of the buckling behavior of steel will improve the finite element prediction as will be reported in upcoming research work.

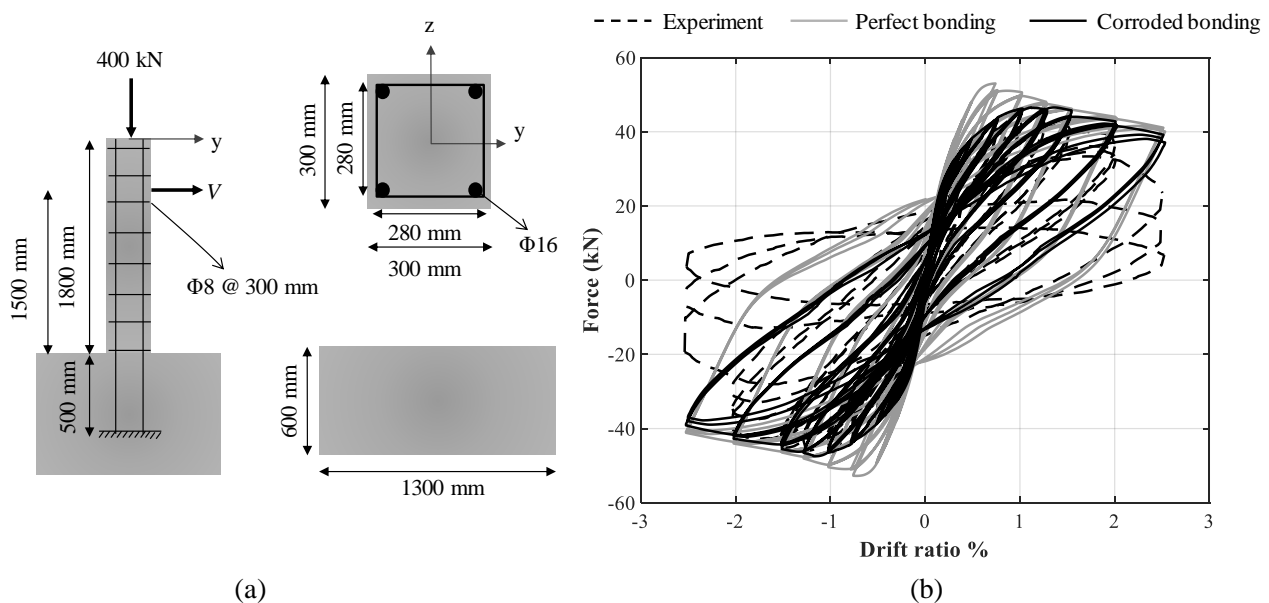


Fig. 5 – (a) Geometry, sections, and axial load, and (b) force-drift ratio hysteresis comparison between FE prediction and experiment for the corroded RC column: Meda column



5. Parametric Study

This section aims at revealing the effect of corrosion on the structural behavior of RC structures through static monotonic and cyclic analyses by varying the corrosion level. The corrosion level is determined based on a time-dependent corrosion model as explained in Section 5.1. The RC column model used for parametric analysis is the one developed for the Meda column but with different levels of corrosion. To gain more insight into the relative importance of corrosion-affected bond-slip, three different cases are studied in comparison with the most important corrosion-affected property (i.e., rebar area reduction): (1) the case with corrosion only reducing the rebar area per Eq. (8); (2) the case with corrosion only deteriorating the bonding between steel rebar and the surrounding concrete as described previously; and (3) the case with corrosion affecting both of the bonding and rebar area. Accordingly, the three cases are referred to as corroded rebar, corroded bonding, and corroded rebar and bonding in this study. The analysis results for these three cases are presented in Section 5.2 and Section 5.3 for the columns under monotonic and cyclic loading, respectively.

5.1 Age-related corrosion levels

To capture the effects of corrosion as an aging phenomenon on the performance of the RC structures, time-dependent corrosion models have been developed under different environmental conditions. This study employs the model developed by [1, 2] to consider reasonable levels of corrosion as an aging effect. The rebar diameter at time t in years, $d_b(t)$, is determined as follows:

$$d_b(t) = \begin{cases} d_{b0} & t \leq T_i \\ d_{b0} - 2\lambda(t - T_i) & T_i < t \leq T_i + \frac{d_{b0}}{2\lambda} \\ 0 & t > T_i + \frac{d_{b0}}{2\lambda} \end{cases} \quad (8)$$

where T_i is the time of corrosion initiation, which can be determined based on Fick's second law of diffusion [2], d_{b0} is the initial rebar diameter, and λ is the corrosion rate, which is equal to 0.0348 mm/year on average for "medium corrosion intensity" situation [1, 2] (e.g., for very aggressive environment such as coastal areas, this rate would be significantly larger). Hence, the corrosion level defined as the mass loss ratio of rebar is calculated based on the rebar area reduction.

5.2 Monotonic results

To evaluate the effect of corrosion on the structural behavior of RC columns, static monotonic pushover analyses are conducted for the corroded RC column with increasing corrosion levels at different ages. According to the age-dependent corrosion model discussed in the previous section, 11 different corrosion levels are considered across a life span of 50 years (i.e., every 5 years), ranging from $K = 0\%$ for a newly built RC column with $t = 0$ (i.e., before the corrosion initiation time $T_i = 2.0$ years for this tested column with concrete cover = 10 mm), up to $K = 38\%$ for an aged RC column with $t = 50$ years. The lateral force-displacement results for the three cases are illustrated in Fig. 6(a) to (c). For comparison purposes, the corresponding results for the pure concrete column (with complete loss of steel rebars) and the perfectly bonded RC column are also shown with the dashed and dotted curves, respectively. In addition, Fig. 6 shows the four limit states as defined corresponding to steel rebar yielding, cover concrete crushing, core concrete crushing, and bond-slip yielding.

Fig. 6 indicates that as the bonding between steel rebars and concrete weakens due to the increasing level of corrosion, the behavior of the column is approaching to the pure concrete column as expected. Specifically, as aging effects get more severe, the contribution of steel would be less significant so that for highly corroded columns, the core concrete crushes before steel yielding. Note that if only the effect of corrosion on rebar area reduction was considered (i.e., without considering the corroded bond-slip as the focus of this study), this effect would not be captured.

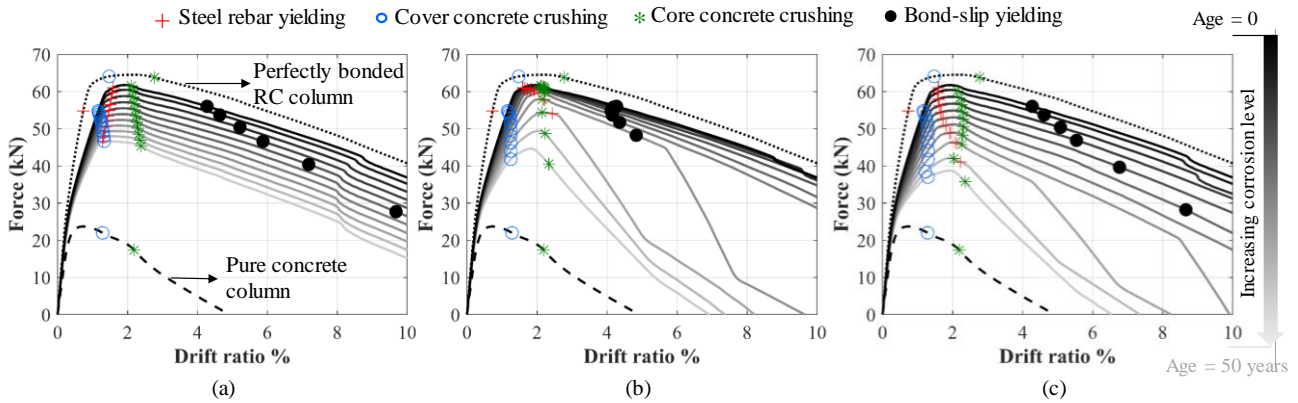


Fig. 6 – Monotonic force-displacement results for RC columns: (a) corroded rebar, (b) corroded bonding, and (c) corroded rebar and bonding

To quantify the effect of corrosion on the performance of the RC column, three different engineering quantities of interest are examined: the secant stiffness reduction ratio, the strength capacity reduction ratio, and the deformation capacity reduction ratio. Here, the secant stiffness is defined based on the first point in which the tangent stiffness is reduced by 20% to measure the stiffness change of the column; the deformation capacity is defined by the normalized displacement corresponding to a drop of 20% in the strength, i.e., non-dimensionalized via being divided by the yield displacement for the uncorroded column. Fig. 7 presents the effect of corrosion level (as indicated by ages) on those quantities for the three cases considered: corroded rebar, corroded bonding, and corroded rebar and bonding. Fig. 7(a) indicates that the secant stiffness reduction at the initial stage is mainly due to rebar area reduction; on the contrary, as the corrosion gets more severe, the corroded bonding would dominate this stiffness reduction (e.g., up to 50%). Fig. 7(b) reveals that the strength capacity is primarily governed by the rebar area rather than bonding, and the corrosion does not significantly affect the strength at low corrosion levels. However, it can be observed that when the corrosion is severe, the bonding would considerably decrease the strength capacity as well. The corrosion can reduce the strength capacity up to about 40% that is *not* negligible. Fig. 7(c) shows the deformation capacity reduction is highly affected by the corroded bonding as well. This reveals that the deformation capacity can be affected more by corroded bonding, although the strength capacity may not be significantly affected by corroded bonding at relatively low corrosion levels.

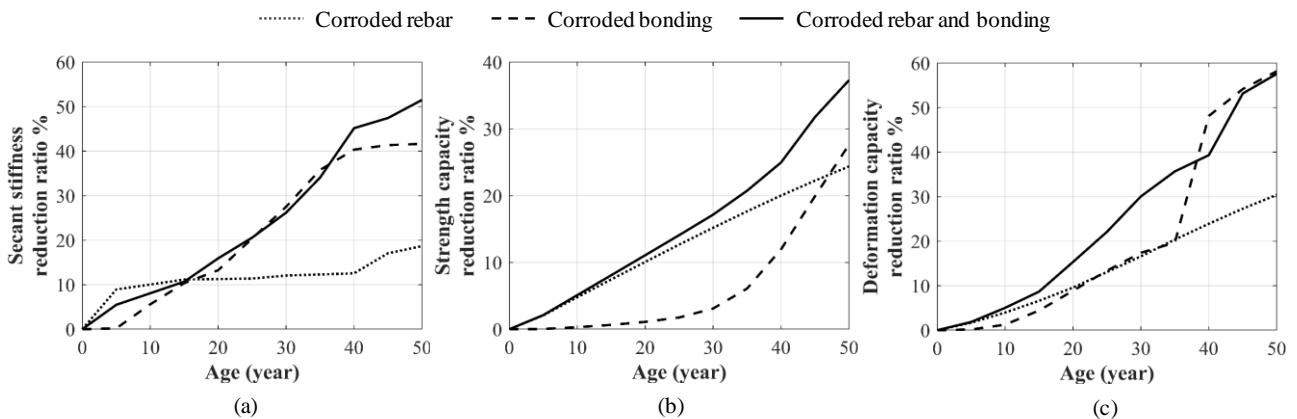


Fig. 7 – Effect of corrosion on different aspects of monotonic behavior of RC columns: (a) secant stiffness, (b) strength capacity, and (c) deformation capability



5.3 Cyclic results

In parallel with the static monotonic pushover analyses, static cyclic pushover analyses are also performed to understand the corrosion effects on the structural performance under cyclic loading. The force-displacement hysteresis for the three different cases aforementioned are demonstrated in Fig. 8(a) to (c). For comparison purposes, the corresponding results for the pure concrete column (with complete loss of steel rebars) and the perfectly bonded RC column are also shown with the dashed and dotted curves, respectively. As seen in Fig. 6(a) to (c), for slightly to moderately corroded columns, the rebar area reduction is the primary factor for the strength degradation. For highly corroded columns, *i.e.*, about aged 40 years and higher, a significant drop can be observed in the strength due to corroded bonding, eventually approaching to the behavior of the pure concrete column. On the other hand, the dissipated energy is mainly reduced because of the corrosion-affected bond-slip.

To further quantify the effect of corrosion on energy dissipation, Fig. 9 shows the dissipated energy loss ratio with respect to the uncorroded normal bonding test for different levels of drift ratios. Comparing Fig. 9(a) to (c) reveals that the reduction in dissipated energy due to corroded bonding can be up to 80% for the worst case while this value would not be more than 30% by considering the corroded rebars with area reduction only. Moreover, the major reduction in dissipated energy occurs at higher levels of deformations. In other words, as the level of deformation increases, the role of corroded bonding gets more significant.

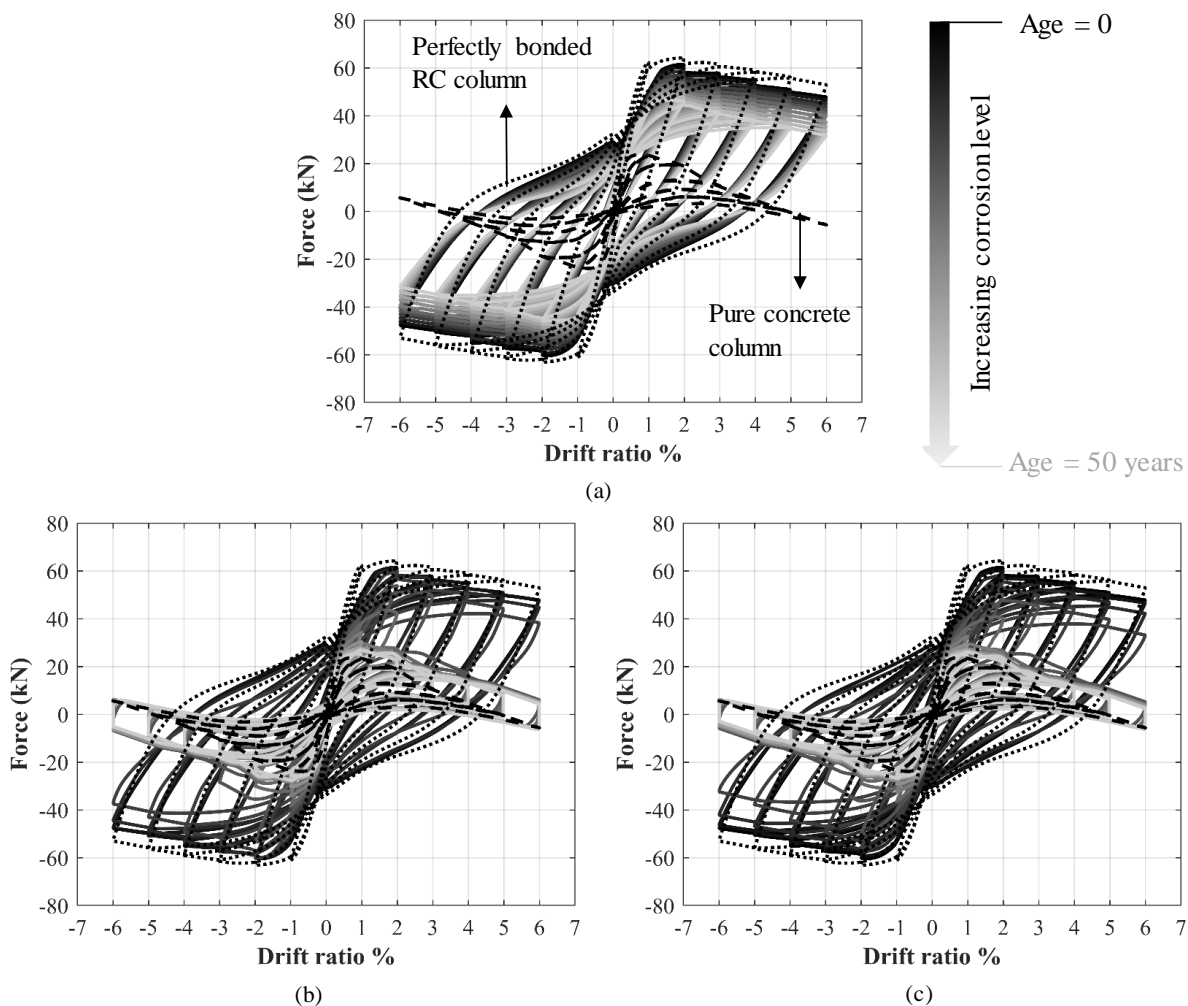


Fig. 8 – Cyclic force-displacement results for RC columns: (a) corroded rebar, (b) corroded bonding, and (c) corroded rebar and bonding

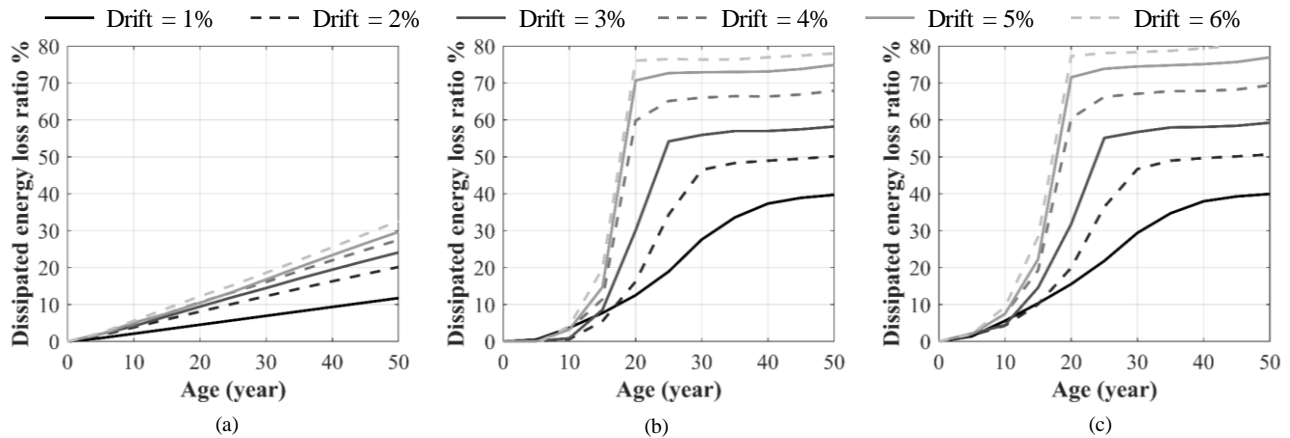


Fig. 9 – Dissipated energy loss ratio for different levels of drift ratio: (a) corroded rebar, (b) corroded bonding, and (c) corroded rebar and bonding

6. Conclusion

This paper studies the effect of corrosion on the nonlinear behavior of reinforced concrete (RC) structures focusing on the impact of imperfect bonding. In order to investigate the true performance of RC structures considering bond-slip between steel rebars and the surrounding concrete, this study first enhances an existing displacement-based fiber beam-column element with bond-slip by accounting for the effect of geometrical nonlinearity. Then, the effect of corrosion is incorporated into bond-slip models, which allows the investigation of corrosion effects on aged RC structures using fiber-based beam-column elements. By considering three different cases: corroded rebar with uncorroded bonding, corroded bonding with uncorroded rebar, and corroded bonding and corroded rebar, the relative importance of the corroded bonding is studied. Comparing the performance of these cases at different ages reaffirms that the performance of RC structures would be significantly degraded as the aging effect gets more severe. In particular, the rebar area reduction is the main factor influencing the strength capacity of the corroded structure until the performance of the structure converges to the pure-concrete structure and hence, the corroded bond-slip controls the strength capacity. On the other hand, the deformation capacity is governed by corroded bond-slip rather than steel rebar section loss. Moreover, the corroded bond-slip has a principal impact on the energy dissipation of RC structures under cyclic loading. Although more studies are needed to further reveal corrosion effect on the RC structures, such as considering dynamic loading and/or pertinent uncertainties, it is a definite conclusion that neglecting the effect of corroded bonding would significantly bias the performance prediction and decision-making for aged RC structures.

7. Acknowledgments

The authors acknowledge the financial support provided by the Natural Sciences and Engineering Research Council (NSERC) in Canada through the Discovery Grant (RGPIN-2017-05556). The first author also would like to acknowledge the Ph.D. Recruitment Scholarship and Graduate Fellowship provided by University of Alberta.

8. References

- [1] Stewart MG, Rosowsky D V (1998): Time-dependent reliability of deteriorating reinforced concrete bridge decks. *Structural Safety*, 20:91–109.
- [2] Ghosh J, Padgett JE (2010): Aging considerations in the development of time-dependent seismic fragility curves. *Journal of Structural Engineering*, 136:1497–511.



- [3] Vu KAT, Stewart MG (2000): Structural reliability of concrete bridges including improved chloride-induced corrosion models. *Structural Safety*, 22:313–33.
- [4] Kivell A, Palermo A, Scott A (2015): Complete model of corrosion-degraded cyclic bond performance in reinforced concrete. *Journal of Structural Engineering*, 141:4014222.
- [5] Vu NS, Yu B, Li B (2016): Prediction of strength and drift capacity of corroded reinforced concrete columns. *Construction and Building Materials*, 115:304–18.
- [6] Mazzoni S, McKenna F, Scott MH, Fenves GL, Jeremic B (2006): Open system for earthquake engineering simulation, User Command Manual. *Pacific Earthquake Engineering Research Center*, Berkeley, California, USA.
- [7] Saatcioglu M, Alsiwat JM, Ozcebe G (1992): Hysteretic behavior of anchorage slip in RC members. *Journal of Structural Engineering*, 118:2439–58.
- [8] Zhao J, Sritharan S (2007): Modeling of strain penetration effects in fiber-based analysis of reinforced concrete structures. *ACI Structural Journal*, 104:133.
- [9] Braga F, Gigliotti R, Laterza M, D'Amato M, Kunnath S (2012): Modified steel bar model incorporating bond-slip for seismic assessment of concrete structures. *Journal of Structural Engineering*, 138:1342–50.
- [10] Monti G, Spacone E (2000): Reinforced concrete fiber beam element with bond-slip. *Journal of Structural Engineering*, 126:654–61.
- [11] Spacone E, Limkatanyu S (2000): Responses of reinforced concrete members including bond-slip effects. *ACI Structural Journal*, 97:831–9.
- [12] Eligehausen R, Popov EP, Bertero VV (1983): Local bond stress-slip relationships of deformed bars under generalized excitations: Experimental results and analytical model. *EERC Report 83-23*, Earthquake Engineering Research Center, University of California, Berkeley, California, USA.
- [13] Murcia-Delso J, Benson Shing P (2015): Bond-slip model for detailed finite-element analysis of reinforced concrete structures. *Journal of Structural Engineering*, 141:4014125.
- [14] Lundgren K, Kettl P, Hanjari KZ, Schlune H, Roman ASS (2012): Analytical model for the bond-slip behavior of corroded ribbed reinforcement. *Structure and Infrastructure Engineering*, 8:157–69.
- [15] Filippou FC, Fenves GL (2004): Methods of analysis for earthquake-resistant structures. *Earthquake Engineering: From engineering seismology to performance-based Engineering*, Y. Bozorgnia and V. V. Bertero, eds., CRC, Boca Raton, Fla., Chap. 6.
- [16] Criesfield MA (1991): *Non-linear finite element analysis of solids and structures*. Vol. 1, Wiley, New York.
- [17] Bousias SN, Verzeletti G, Fardis MN, Gutierrez E (1995): Load-path effects in column biaxial bending with axial force. *Journal of Engineering Mechanics*, 121:596–605.
- [18] Ayoub A (2006): Nonlinear Analysis of Reinforced Concrete Beam-Columns with Bond-Slip. *Journal of Engineering Mechanics*, 132:1177–86.
- [19] Meda A, Mostosi S, Rinaldi Z, Riva P (2014): Experimental evaluation of the corrosion influence on the cyclic behavior of RC columns. *Engineering Structures*, 76:112–23.
- [20] Coronelli D, Gambarova P (2004): Structural assessment of corroded reinforced concrete beams: modeling guidelines. *Journal of Structural Engineering*, 130:1214–24.
- [21] Stewart MG (2009): Mechanical behavior of pitting corrosion of flexural and shear reinforcement and its effect on structural reliability of corroding RC beams. *Structural Safety*, 31:19–30.
- [22] Mander JB, Priestley MJN, Park R (1988): Theoretical stress-strain model for confined concrete. *Journal of Structural Engineering*, 114:1804–26.